This is a draft of the accepted Journal on IET MAP;
ISSN 1751-8725; August 2015
doi: 10.1049/iet-map.2014.0736
www.ietdl.org

The Design of a Uniplanar Printed Triple Band-Rejected UWB Antenna using Particle Swarm Optimization and the Firefly Algorithm

Husham J. Mohammed[1,2], Abdulkareem S. Abdulla[1], Ramzy S. Ali[1], Raed A. Abd-Alhameed[2], Yasir I. Abdulraheem[1,2] and James M. Noras[2]

[1]Dept. of Electrical Engineering, University of Basrah, Basrah, Iraq

[2]School of Engineering and Informatics, University of Bradford, Bradford, UK

Abstract: A compact planar monopole antenna is proposed for ultra-wideband applications. The antenna has a microstrip line feed and band-rejected characteristics and consists of a ring patch and partial ground plane with a defective ground structure of rectangular shape. An annular strip is etched above the radiating element and two slots, one C-shaped and one arc-shaped, are embedded in the radiating patch. The proposed antenna has been optimized using bio-inspired algorithms, namely Particle Swarm Optimization and the Firefly Algorithm, based on a new software algorithm (Antenna Optimizer). Multi-objective optimization achieves rejection bands at 3.3 to 3.7 GHz for WiMAX, 5.15 to 5.825 GHz for the 802.11a WLAN system or HIPERLAN/2, and 7.25 to 7.745 GHz for C-band satellite communication systems. Validated results show wideband performance from 2.7 to 10.6 GHz with S_{11} < -10 dB. The antenna has compact dimensions of 28 × 30 mm^2. The radiation pattern is comparatively stable across the operating band with a relatively stable gain except in the notched bands.

Keywords: Particle Swarm Optimization, Firefly Algorithm, Ultra Wideband Antenna, Planer Antenna, Notched band.

This is a draft of the accepted Journal on IET MAP;
ISSN 1751-8725; August 2015
doi: 10.1049/iet-map.2014.0736
www.ietdl.org

1 Introduction

Ultra-wideband (UWB) technology is increasingly important in applications such as sensor networks, medical imaging, multimedia communications, precision localization systems, and ground-penetrating radar [1-6]. Due to its low complexity, ease of connection, and high data transmission rates, UWB has been used in many devices such as high definition TVs, laptops, wearable bio-medical sensors and digital cameras. In such applications, the antenna is a critical component, required to be small enough to be integrated with other RF circuits or embedded within wireless devices, with low cost, and stable radiation characteristics over a wide impedance bandwidth.

The 3.2 GHz to 10.6 GHz frequency band for unlicensed UWB radio communication was released in February 2002 by the US Federal Communications Commission [7]. This band encompasses several existing narrow-band communication systems, such as WLAN systems operating in the 5.15 GHz to 5.825 GHz band, C-band satellite systems in the 7.25 GHz to 7.745 GHz band, and WiMAX operating in the 3.3 GHz to 3.7 GHz band [8]; these narrow-band systems potentially can interfere with UWB systems. To suppress interference, it is possible to use a spatial filter [9]. Nevertheless, this method would increase the cost and complexity of the system, and would take up space when integrated with other microwave circuitry. Another way to filter out these narrow band systems from UWB applications is to design antennas with band-notch properties.

Various impedance matching principles are presented in the literature, such as impedance matching optimization through an embedded slot in the radiator [10-12]. In designing slots [13], the authors used the guided wavelength:

$$\lambda_{\mathrm{g}} = \frac{\lambda_{\mathrm{notch}}}{\sqrt{\varepsilon_{\mathrm{eff}}}} \tag{1}$$

This is a draft of the accepted Journal on IET MAP;
ISSN 1751-8725; August 2015
doi: 10.1049/iet-map.2014.0736
www.ietdl.org

$$\varepsilon_{\text{eff}} = \frac{\varepsilon_{\text{r}} + 1}{2} \tag{2}$$

where λ_{g} and λ_{notch} are the guided and notch wavelengths respectively. ε_{r} is the relative permittivity of the substrate.

Another technique proposed used parasitic patches to achieve a notched band [14]. Other examples include introducing an H-shaped slot close to the feeding point to filter out the WLAN band between 5.15 to 5.35 GHz [15], embedding CSRR slots and open circuited stubs on the radiating elements to notch the WiMAX 3.3 to 3.7 GHz band and the WLAN 5.15 to 5.8 GHz band [16], inserting two elliptic single complementary split-ring resonators to filter out the WiMAX 3.3 to 3.8 GHz band and WLAN 5.15 to 5.85 GHz band [17], or placing two strips on the ground plane to reject the WLAN band operating at 5.15 to 5.85 GHz for portable UWB applications [18].

When considering global optimization methods for antenna designs, bio-inspired algorithms such as genetic algorithms (GA) [19] and Particle Swarm Optimization (PSO) [20, 21], have been commonly used in the creation of design techniques that can satisfy constraints which would be otherwise unattainable.

This paper compares PSO with the Firefly Algorithm (FA), a population-based adaptive stochastic optimization technique [22]. The application is the multi-objective optimization of a uniplanar printed triple band-rejected UWB antenna. Current electromagnetic solvers do have some integrated optimization tools that can aid antenna designers, but most of these tools do not allow designers to specify objective functions. With optimization problems requiring difficult settings of objective functions, it would be desirable to express objective functions in a programming environment. In the work reported here, the particular algorithms have been developed into novel software, used to design and optimize a simple

This is a draft of the accepted Journal on IET MAP;
ISSN 1751-8725; August 2015
doi: 10.1049/iet-map.2014.0736
www.ietdl.org

and compact UWB.

2 Bio-inspired Optimization

2.1 Particle Swarm Optimization

Like the genetic algorithm (GA), PSO is a population-based adaptive stochastic optimization method, but differs in having no evolutionary factors such as crossover, mutation or selection: the method is based on the collective swarm intelligence observed in the social behaviour of birds, fish, bees, etc. [23].

In PSO, the particles represent potential solutions to the optimization problem, with an associated location and velocity; a fitness function is used to evaluate and compare locations. Each particle keeps track of its own best location, and the global location of the entire swarm. If a particle's current position has a better fitness value than its previous best location, the best location is updated by the current position: if any particle has a best position better than the current global position, that is also replaced.

In this paper the application of the PSO is based on [20], where the update equations of velocity and position are given by:

$$v_i^{k+1} = w^k v_i^k + c1\, r_{1,i}^k \left(p_i^k - x_i^k \right) + c2\, r_{2,i}^k \left(g_i^k - x_i^k \right) \tag{3}$$

$$x_i^{k+1} = x_i^k + (v_i^{k+1}\, \Delta t) \tag{4}$$

where *k* refers to the current iteration, i is the index of each particle, with v_i^k and x_i^k current velocities and positions respectively. w^k contains the inertial weights which set the effect of the particle's previous trajectory. p_i^k gives each particle's best location, and g_i^k is the global optimum. The parameters c2 and c1 are the social weight, and the cognitive weight, which determine whether a particle has a tendency towards the best position or towards the global position. More precisely, the cognitive parameter relates to the experience of

This is a draft of the accepted Journal on IET MAP;
ISSN 1751-8725; August 2015
doi: 10.1049/iet-map.2014.0736
www.ietdl.org

each particle with respect to its best performance so far, while the social parameter relates to the best position found by either the whole swarm or a particle's neighbourhood. $r_{1,i}^{k}$ and $r_{2,i}^{k}$ are arbitrary numbers uniformly distributed in [0,1], and Δt is the time step, normally set to unity.

2.2 Firefly Optimization

The Firefly Algorithm (FA) was developed by Yang [22, 24], and is proposed for several different optimization applications. It is a population-based adaptive stochastic optimization method like PSO, inspired by the flashing patterns and characteristics of fireflies. The flashes are to attract possible prey and to communicate or attract mating partners. Yang idealized some rules with respect to the real behaviour of fireflies:

1) All fireflies are unisex: regardless of their sex, all fireflies are attracted to each other.
2) Attractiveness is proportional to brightness, brightness decreasing with increasing separation distance. A less bright firefly will move towards a brighter one; if there is no particularly bright attractor, movement is random.
3) The firefly's brightness is set by the cost function. In the simplest case, at a particular position *x*, the brightness *h(x)* of a firefly is chosen as

$$h(x) = 1 / f(x)$$

where f(x) refers to the cost function.

The firefly's attractiveness β depends on its brightness. Nevertheless, this attractiveness is relative, as judged by other fireflies. Therefore, it will be a function of the separation distance r_{ij} between firefly *i* and firefly *j*. The separation distance between any two fireflies *i* and *j* at x_i and x_j, respectively, is the Cartesian distance r_{ij} given by:

This is a draft of the accepted Journal on IET MAP;
ISSN 1751-8725; August 2015
doi: 10.1049/iet-map.2014.0736
www.ietdl.org

$$r_{ij} = \|x_i - x_j\| = \sqrt{\sum_{k=1}^{p} (x_{i,n} - x_{j,n})^2} \quad (5)$$

where $x_{i,n}$ is the nth component of the spatial coordinate x_i of firefly *i*, and *p* is the dimension of each x_i and x_j. With a fixed light absorption factor γ for a given medium, β varies with r_{ij}:

$$\beta(r) = \beta_0 e^{-\gamma r_{ij}^2} \quad (6) \quad (6)$$

where β_0 is the attractiveness at r_{ij}= 0

Firefly *i* is moved by attraction to another firefly *j* that should be more brighter, attractive or repulsed by firefly *j* that has less bright. This movement is given by:

$$x_i^{m+1} = x_i^m + \beta_0 e^{-\gamma r_{ij}^2}\left(x_j - x_i^m\right) + \alpha \left(rand - \frac{1}{2}\right) \quad (7)$$

where *m* refers to the current iteration and x_i is the current position. The second term gives the effect of attraction whereas the third term expresses the randomization: α is the randomization factor, α ∈ [0, 1]. *rand* is an arbitrary number uniformly distributed in [0, 1].

3 Single Band-rejected Antennas Design

3.1 Primitive Antenna

Fig.1(a) and (b) show the geometry of the primitive annular patch antenna, which is printed on one side of an FR4 substrate with a relative dielectric constant of 4.4, thickness 1.6 mm, and dimensions 30 x 30 mm^2. The radiation element is the annular patch that is fed by a microstrip line of width 3 mm and length 12 mm. The inner r_1 and outer r_2 radius values are 3 mm and 8 mm respectively. A partial ground is printed on the other side of the

This is a draft of the accepted Journal on IET MAP;
ISSN 1751-8725; August 2015
doi: 10.1049/iet-map.2014.0736
www.ietdl.org

substrate with a width of 30 mm and length 12 mm. A defective ground structure is used as a rectangular shape with dimensions of *ws* × *ls* mm^2, where *ws* and *ls* are equal to 2 mm and 1 mm respectively.

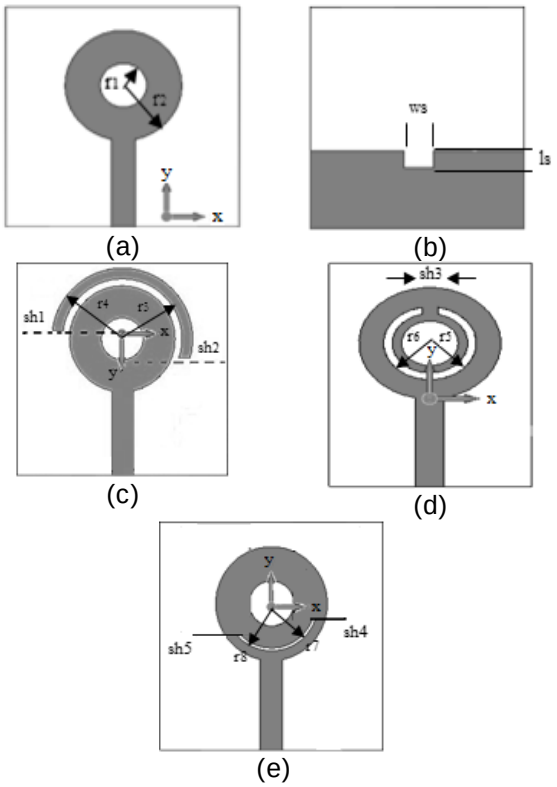

Fig. 1 Geometry of the (a) Primitive antenna (front view), (b) Primitive antenna (bottom view), (c) WLAN band-rejected antenna, (d) WiMAX band-rejected antenna, and (e) C-band band-rejected antenna.

3.2 Antenna with Parasitic Annular Strip

WLAN radio signals already occupy specific frequencies in the UWB band, between 5.15 GHz and 5.825 GHz, and so might interfere with UWB systems unless band-rejection were introduced.

Fig. 1(c) shows the antenna geometry. A semi-circular annular strip with an inner radius r_3 of 8.5 mm and outer radius r_4 of 9.7 mm has been etched above the annular patch, resulting in high impedance at the particular notch frequency. The length of this strip is bounded by two plane edges, sh1 and sh2. The effective length of the annular strip is 33.2 mm which should equal the guided wavelength for the required notch frequency of 5.5 GHz, as calculated by Equation (1). Thus, the corresponding values of sh1 and sh2 will be

This is a draft of the accepted Journal on IET MAP;
ISSN 1751-8725; August 2015
doi: 10.1049/iet-map.2014.0736
www.ietdl.org

approximately 1 mm and 5.3 mm respectively.

3.3 Antenna with a C-Shaped Slot

WiMAX operates in the range of 3.3 GHz to 3.7 GHz and so might interfere with UWB devices. A C-shaped slot is cut in the primitive antenna as shown in Fig. 1(d), intended to minimize potential interference. The values of the inner radius r_5 and outer radius r_6 are 4 mm and 4.5 mm respectively. The length of the slot is bounded by the plane edge sh3. The effective length of the C-shaped slot should be around half the guided wavelength at the required notch frequency of 3.45 GHz, calculated using Equation (1) as 26.5 mm. Therefore, sh3 will be approximately 3 mm.

3.4 Antenna with an Arc-Shaped Slot

C-band satellite systems operate at 7.25 GHz to 7.745 GHz, another potential source of interference, requiring a band-notched characteristic at these frequencies. Fig. 1(e) shows the geometry of the modified antenna. An arc-slot with an inner radius r_7 and outer radius r_8 of 5.9 mm and 6.4 mm respectively has been embedded in the radiating element, which leads to high impedance at the notch frequency. The length of this strip is bounded by two plane edges sh4 and sh5. The effective length of the arc-slot should be around half the guided wavelength of the required notch frequency 7.4 GHz given by Equation (1), calculated as 12.3 mm. Therefore, the values of sh4 and sh5 will be approximately 2 and 4 mm respectively but in the negative direction of the y-axis.

The simulated input reflection coefficients of the primitive and single band-notch antennas are shown in Fig. 2.

4 Parameters Study

To investigate the key parameters, the antenna with parasitic annular strip is now

This is a draft of the accepted Journal on IET MAP;
ISSN 1751-8725; August 2015
doi: 10.1049/iet-map.2014.0736
www.ietdl.org

analyzed as an example.

Fig. 3 shows the reflection coefficient curves of the antenna for various values of sh1, keeping sh2 at 1 mm. It is noticed that as sh1 increases from 2 mm to 6 mm, the centre frequency of the notch band decreases from 5.78 GHz to 5.08 GHz.

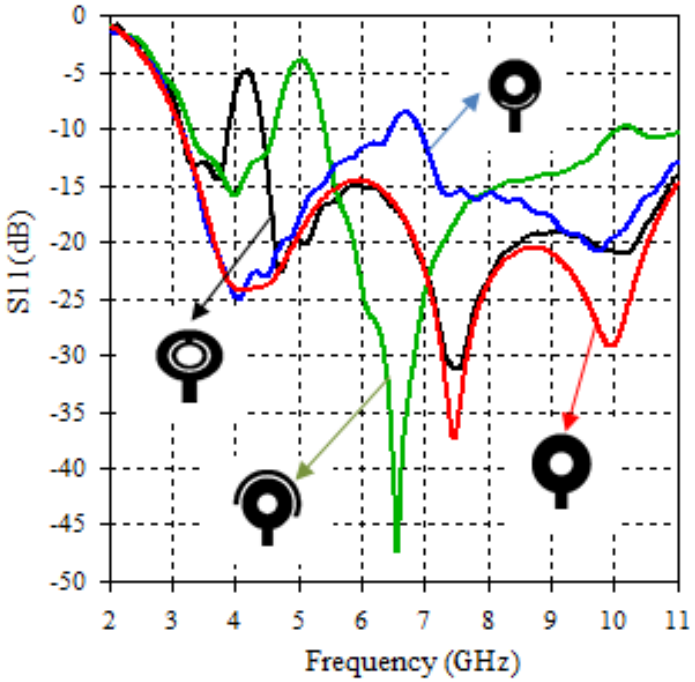

Fig. 2 Simulated input reflection coefficients

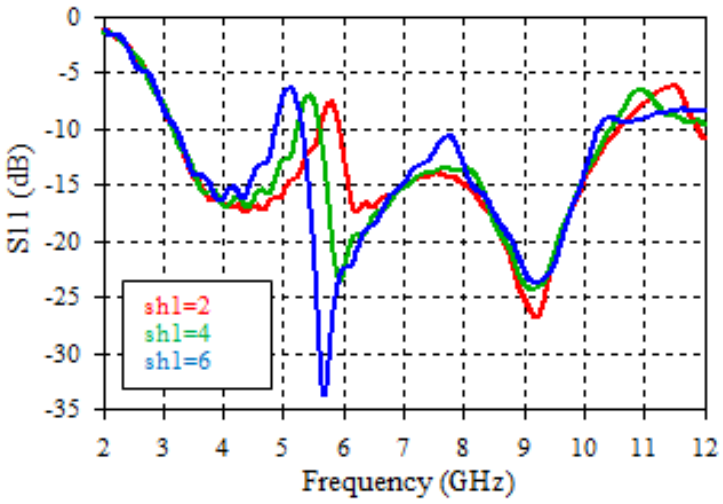

Fig. 3 Reflection coefficients for different values of sh1

Fig. 4 illustrates the reflection coefficient curves with sh1 = 0, for sh2 varying from 2 mm to 6 mm, where the centre frequency of the notch band varies from 6 GHz to 5.2 GHz. Next, Fig. 5 illustrates the reflection coefficient curves with r_3 = 8.5 mm for r_4

This is a draft of the accepted Journal on IET MAP;
ISSN 1751-8725; August 2015
doi: 10.1049/iet-map.2014.0736
www.ietdl.org

varying from 8.8 mm to 9.6 mm, where the notched bandwidth increased. The effect of sh1 has the same type of effect as sh2 because both are related to the length of the parasitic element. From the above parametric study, it can be concluded that the centre frequency of the notch band can be controlled by varying the values of sh1 and sh2. The width of the notch band can be controlled by changing the width of the parasitic element.

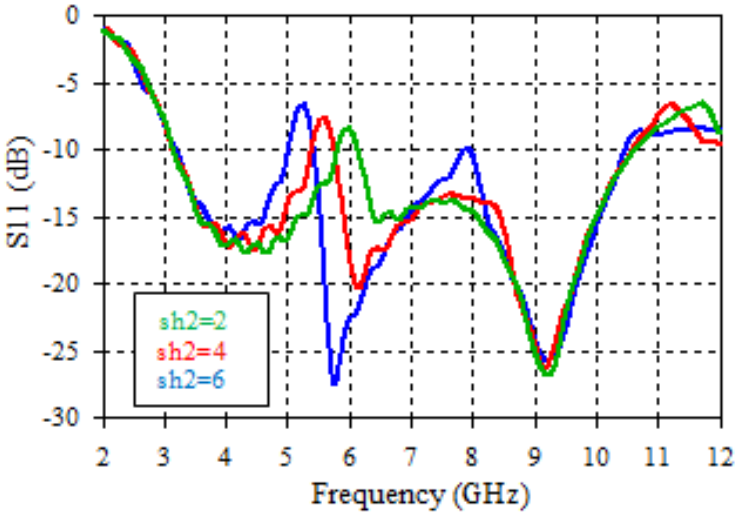

Fig. 4 Reflection coefficient for different values of sh2

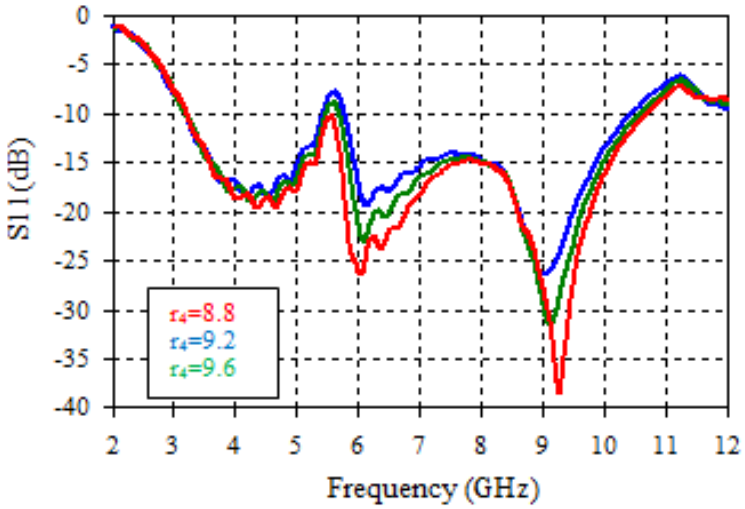

Fig. 5 Reflection coefficient for different values of r4

5 Triple Band-rejected Antenna Design

5.1 Antenna Geometry

Fig. 6 shows the composite geometry of the triple band-notch UWB antenna which is the combination of the previous three structures. Comparing with Fig.2 it can be

This is a draft of the accepted Journal on IET MAP;
ISSN 1751-8725; August 2015
doi: 10.1049/iet-map.2014.0736
www.ietdl.org

seen that the resulting notch band of each antenna can be above or below that of the individual cases, and the values of S_{11} in the notched bands is not enough to prevent interference with the narrow band system. So, the notching frequencies need to be tuned, and their return loss values improved: these targets can be expressed as objective functions for the bio-inspired optimization.

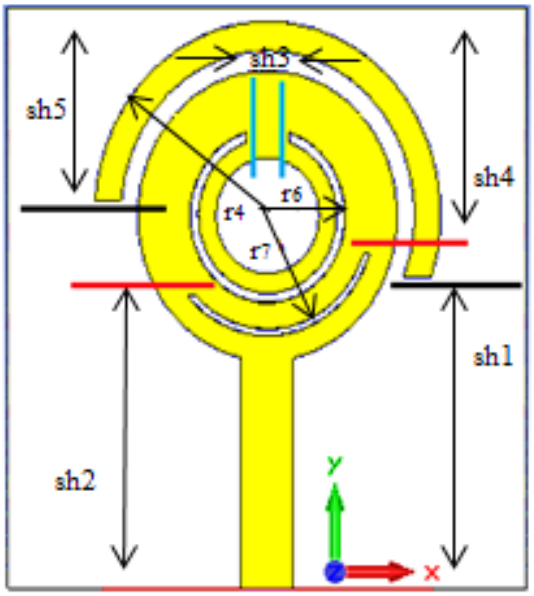

Fig. 6 Geometry of the triple band-notch antenna

5.2 Objective Functions

Two objectives are to be satisfied. Each objective with its corresponding cost function is described below, and then the separate cost functions are combined into a single fitness function.

$$\mathbf{Gf1} = \sum_{f_1}^{f_2} \boldsymbol{p(f)} + \sum_{f_3}^{f_4} \boldsymbol{p(f)} + \sum_{f_5}^{f_6} \boldsymbol{p(f)} \tag{8}$$

$$\text{where } p(f) = \begin{cases} 0 \; for \; S_{11} \geq -4 \\ -S_{11} \; for \; S_{11} < -4 \end{cases}$$

$$\mathbf{Gf2} = \sum_{f_2+0.01}^{f_3-0.01} k(f) + \sum_{f_4+0.01}^{f_5-0.01} k(f) + \sum_{f_6+0.01}^{f_7} k(f) \tag{9}$$

This is a draft of the accepted Journal on IET MAP;
ISSN 1751-8725; August 2015
doi: 10.1049/iet-map.2014.0736
www.ietdl.org

$$\text{where } k(f) = \begin{cases} -S_{11}\ for\ S_{11} \geq -10 \\ 0\ for\ S_{11} < -10 \end{cases}$$

$$\mathbf{Gf} = \left| \frac{1}{(\mathbf{Gf1} + \mathbf{Gf2}) + 1} - 1 \right| \quad (10)$$

Here S_{11} is the input reflection coefficient loss in dB, f_1 and f_2 are the lower and upper frequencies for the WiMAX band, f_3 and f_4 are the lower and upper frequencies for the WLAN band, f_5 and f_6 are the lower and upper frequencies for the C-band satellite communication systems, and f_7 is the highest frequency of the UWB band. N is the number of frequency samples taken between f_1 and f_7. Gf1 is the cost function responsible for a band's rejection whereas Gf2 is the cost function responsible for making the reflection coefficient in the other bands less than –10 dB. Gf is the overall fitness function. We can conclude from the conditions of Equations 8 and 9 that the best possible fitness value is 0. However, if any other antenna parameters (example peak gain or specific radiation pattern in plane) are described well and merged into the specific overall fitness function given in (10), subject to appropriate weightings, then it is possible to improve or modify that parameter or parameters. The present work has not considered such an extended optimisation procedure.

5.3 Antenna Optimizer Software

For the optimization, an interface between MATLAB [25] and the electromagnetic simulator CST Microwave Studio [26], called "Antenna Optimizer", has been created, based on the graphical user interface tools of MATLAB. This enables MATLAB to control the optimization in an automated design process, as shown in Fig. 7.

6 Simulated and Measured Results

The parameter study identified some of the key antenna parameters for the notching

This is a draft of the accepted Journal on IET MAP;
ISSN 1751-8725; August 2015
doi: 10.1049/iet-map.2014.0736
www.ietdl.org

characteristics, to be used in optimization with PSO and the FA. The parameters' domain limits are given in Table 1, and the other parameters needed by the particular algorithms are given in Table 2. The population size, number of variables, variable limits, and number of iterations are the same for PSO and the FA.

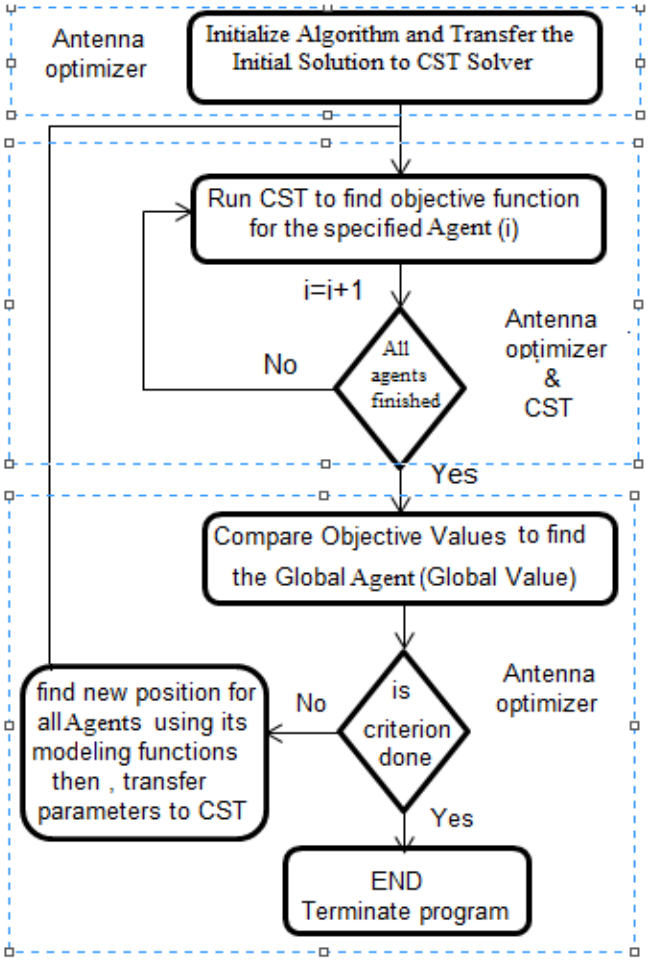

Fig. 7 Automated design process

Running on a HP Compaq 8200 Elite CMT PC with 16 GB RAM and 3.4 GHz CPU, a single fitness function evaluation took some 7 to 10 minutes and an entire algorithm optimization run took 3 to 4 hours. The fitness functions of the particular algorithms are shown in Fig. 8. The FA optimized design reached a fitness value of 0.036 at step 345, whereas for the PSO the fitness value was 0.066 at step 361.

Fig. 8 gives a clear view of the behaviour of the agents throughout the search domain, whereas Fig. 9 shows the best agent fitness values in each iteration of the specific

This is a draft of the accepted Journal on IET MAP;
ISSN 1751-8725; August 2015
doi: 10.1049/iet-map.2014.0736
www.ietdl.org

algorithms.

Table 1: Values of antenna parameter limits

Parameters	Min_Values (mm)	Max_Values (mm)
sh1	-2	2
sh2	0	5
sh3	0	4
sh4	-6	0
sh5	-5	0
r_4	8.8	10
r_6	4.5	5.3
r_8	6	7
ws	1	6
ls	1	5

Table 2: Algorithms parameter values

Algorithm	Parameter	Value
PSO	Population size	20
	N. Variables	10
	N. Iterations	20
	c1	2
	c2	2
	w	0.65
	Steps= Population size * N. Iterations	400
FA	γ	1
	α	0.5
	β	0.2

From Fig. 8 and 9, it can be seen that the FA is faster than PSO and achieved better fitness values. The behaviour of FA agents' fitness values is more stable than with PSO: fireflies worked almost individually and grouped more closely around each optimal point without hopping around as in PSO.

Based on the FA optimal parameters shown in Table 3, the antenna was fabricated and is shown in Fig. 10. S_{11} was measured using the HP 8510C Network Analyzer. Fig. 11 displays the measured and simulated S_{11} results of the designed antenna, showing a wideband performance from 2.7 GHz to 10.6 GHz for $S_{11} < -10$ dB.

This is a draft of the accepted Journal on IET MAP;
ISSN 1751-8725; August 2015
doi: 10.1049/iet-map.2014.0736
www.ietdl.org

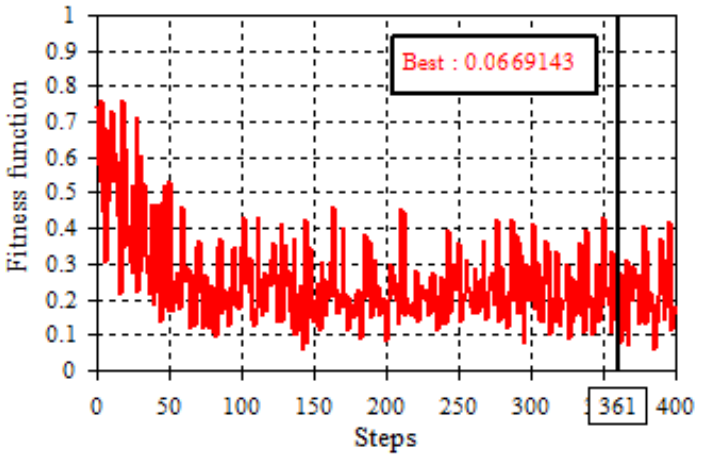

(a)

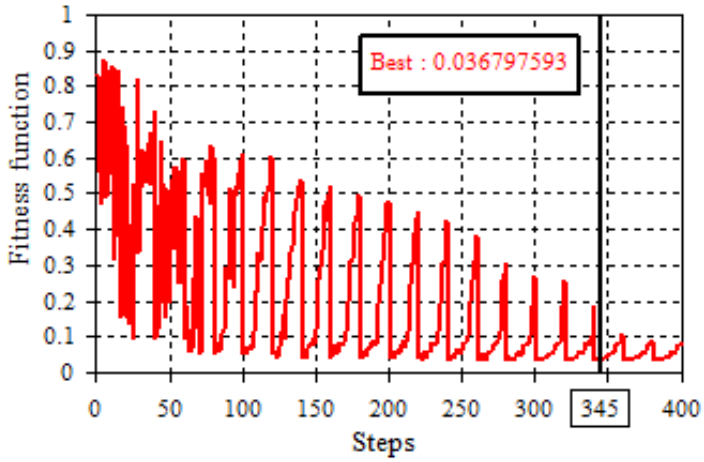

(b)

Fig. 8 Fitness functions of (a) PSO, and (b) FA

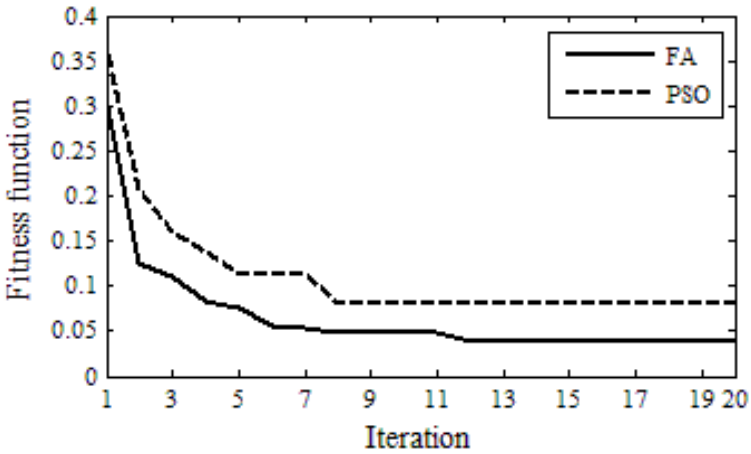

Fig. 9 Optimal agents fitness values for PSO and the FA

The normalized simulated and measured radiation patterns in the *xz* and *yz* plane at 4.11 GHz, 6.11 GHz, 8.3 GHz and 3.6 GHz are shown in Fig. 12. E_{φ} represents the co-polarization properties, and E_{θ} represents the cross-polarization properties. The cross-

This is a draft of the accepted Journal on IET MAP;
ISSN 1751-8725; August 2015
doi: 10.1049/iet-map.2014.0736
www.ietdl.org

polarization dimensions are smaller than the co-polarization dimension in the *xz*-plane at the resonances 4.1 GHz, 6.11 GHz, 8.3 GHz and 3.6 GHz, whereas the co-polarization dimensions are smaller than the cross-polarization dimension in the *yz*-plane. The antenna has nearly omnidirectional radiation patterns.

Table 3: Optimal values of antenna parameters

Parameters	Optimal values (mm)
sh1	0.248459
sh2	3.661857
sh3	2.492596
sh4	-4.858249
sh5	-1.656952
r_4	9.898860
r_6	4.906965
r_8	6.623525
Ws	3.569930
Ls	2.993580

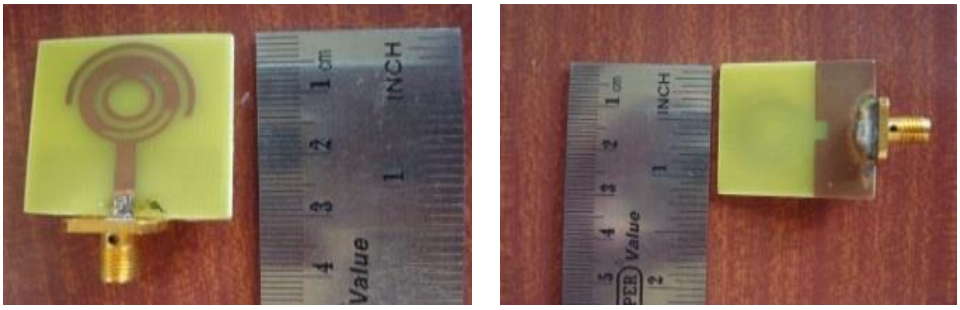

(a) (b)

Fig. 10 Fabricated antenna (a) front view and (b) rear view

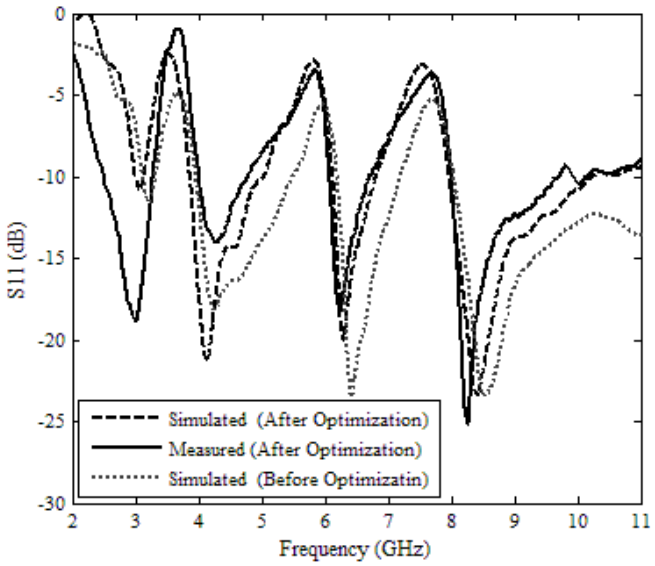

Fig. 11 Simulated and measured reflection coefficients

This is a draft of the accepted Journal on IET MAP;
ISSN 1751-8725; August 2015
doi: 10.1049/iet-map.2014.0736
www.ietdl.org

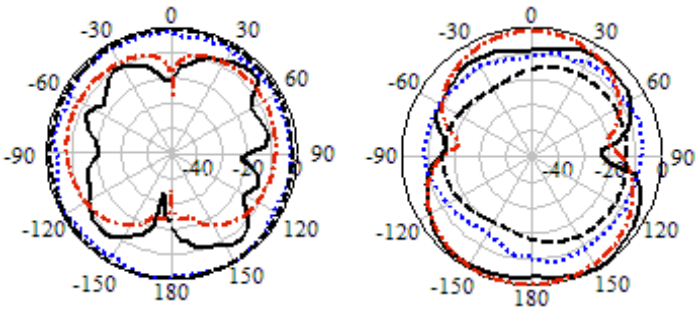

4.11 GHz

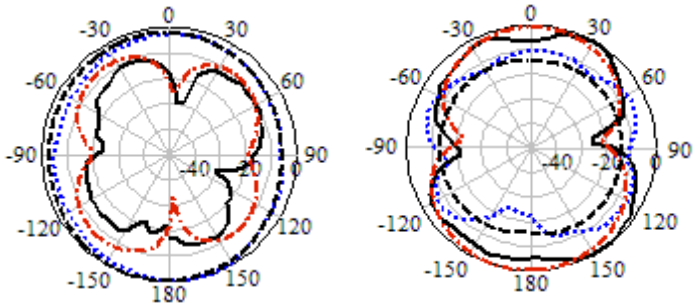

6.11 GHz

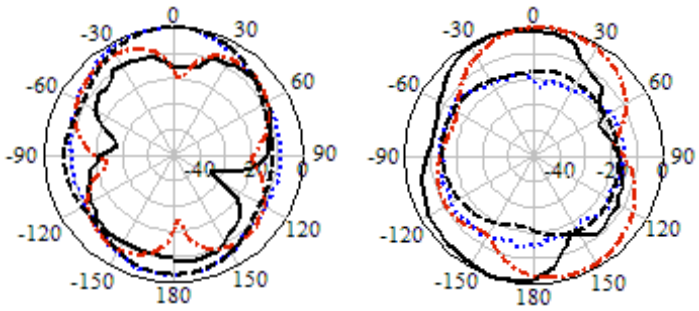

8.3 GHz

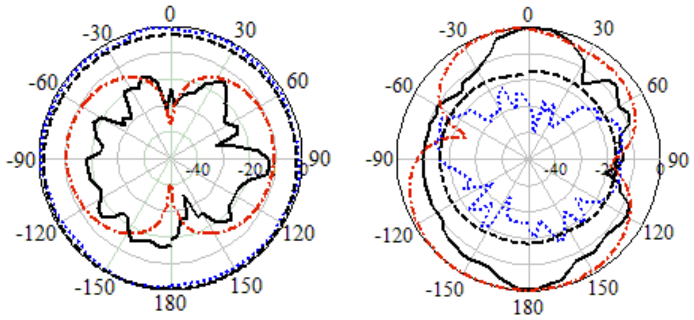

3.6 GHz

Fig. 12 Simulated and measured radiation patterns (a) in *xz*- plane and (b) in *yz*- plane. Simulated E_Θ: dashed-dotted line. Measured E_Θ: solid line. Simulated E_φ: dashed line. Measured E_φ: dotted line.

The measured and simulated gains from 2 GHz to 11 GHz, see Fig. 13, show that the gain decreases sharply around 3.55 GHz, 5.5 GHz, and 7.2 GHz. Outside the notch bands gains varying less than 5.8 dB are achieved, indicating stable performance across the

This is a draft of the accepted Journal on IET MAP;
ISSN 1751-8725; August 2015
doi: 10.1049/iet-map.2014.0736
www.ietdl.org

operating bands.

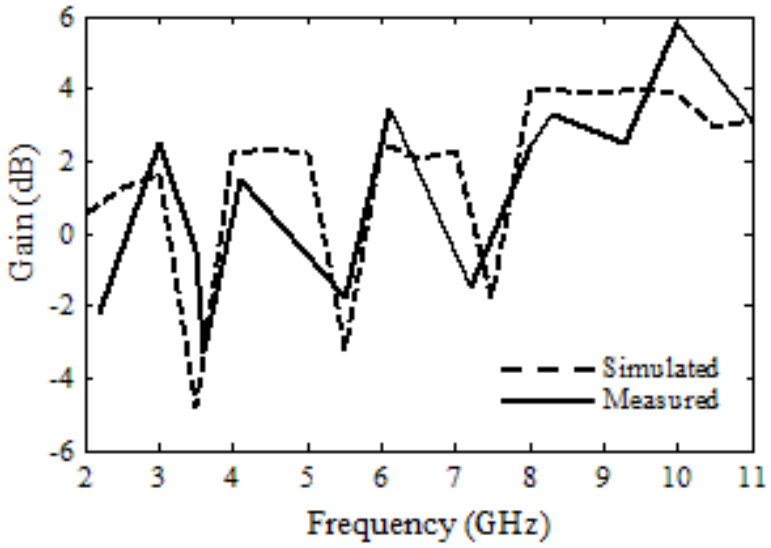

Fig. 13 Simulated and measured realized gain versus frequency

7 Conclusions

This study presents a compact, simple microstrip-fed printed monopole UWB antenna with triple band-rejected facility. To obviate possible interference between UWB systems and narrowband WLAN, WiMAX, and C-band satellite communication systems, an annular patch as a parasitic element, a C-shaped slot and an arc-slot are added for band rejection. Positioning of the desired rejected bands was achieved by optimizing the antenna parameters using PSO and the FA based on novel software (Antenna Optimizer Software). The FA, which has not been applied to this type of problem before, gives a better result than PSO.

Both simulations and measurements show that the antenna has triple notched bands over an ultra-wide operation band, combined with a good radiation pattern and useful gain. The compact size, simple structure and excellent performance of the antenna make it a good candidate for various UWB applications.

This is a draft of the accepted Journal on IET MAP;
ISSN 1751-8725; August 2015
doi: 10.1049/iet-map.2014.0736
www.ietdl.org

Acknowledgments:

This work was supported in part by the United Kingdom Engineering and Physical Science Research Council (EPSRC) under Grant EP/E022936A, TSB UK under grant application KTP008734 and the Iraqi Ministry of Higher Education and Scientific Research.

References:

1 M.E. Bialkowski, W.C. Khor, and S. Crozier, “A planar microwave imaging system with step-frequency synthesized pulse using different calibration methods", *Microw. Opt. Technol. Lett.*, vol.48, pp.511-516, 2006.

2 A.S. Turk, and H. Nazli, "Hyper-wide band TEM horn array design for multi band impulse ground penetrating radar", *Microw. Opt. Technol. Lett.*, vol.50, pp.76-81, 2008.

3 F. Viani, L. Lizzi, R. Azaro, and A. Massa, "A miniaturized UWB antenna for wireless dongle devices", *IEEE Antennas Wireless Propag. Lett*., vol.7, pp.714-717, 2008.

4 M.T. Islam, N. Misran, and A.T. Mobashsher, “Compact dual band microstrip antenna for ku-band application”, *Inform. Technol. J*., vol.9, pp.354-358, 2009.

5 H.D. Mei, and Z.Q. Yu, “Impulse radio ultra-wide-band through wall imaging radar based on multiple-input multiple-output antenna arrays", *Inform. Technol. J*., vol.9, pp.782-789, 2010.

6 M.T. Islam, R. Azim, and N. Misran, "Linear polarized patch antenna for satellite communication", *Inform. Technol. J*., vol.9, pp.386-390, 2010.

7 Federal Communications Commission, Washington, DC, "FCC report and order on ultra-wideband technology", 2002.

This is a draft of the accepted Journal on IET MAP;
ISSN 1751-8725; August 2015
doi: 10.1049/iet-map.2014.0736
www.ietdl.org

8 C. C. Lin, P. Jin, and R. W. Ziolkowski, “Single, dual and tri-band-notched ultra-wideband antennas using capacitively loaded loop resonators", *IEEE Trans. Antennas Propag*., vol.60, no.1, pp.102-109, Jan. 2012.

9 J. Yeo, and R. Mittra, "A novel wideband antenna package design with a compact spatial notch filter for wireless applications", *Microw. Opt. Technol. Lett.*, vol.35, pp.455-460, 2002.

10 P. Xu, Z. Yan, T. Zhang, and X. Yang, "Broadband Circularly Polarized Slot Antenna Array with Fan-Shaped Feed Line and L-Shaped Grounded Strips”,*Progress In Electromagnetics Research Letters*, Vol.44, pp.125-131, 2014.

11 Ming-Chun Tang and Richard W. Ziolkowski, "Compact Hyper-band Printed Slot Antenna Design and Experiments”, The 8th European Conference on Antennas and Propagation (EuCAP), pp.594-596, 2014.

12 B. Sahu and P. Jain, "Dual Band Antenna Design with Improved Result for Mobile and Satellite Application”, *International Journal of Electronics and Communication Engineering,* vol.1, no.7, pp.50-55, Sep. 2014.

13 T. D. Nguyen, D. H. Lee, and H. C. Park, "Design and analysis of compact printed triple band-notched UWB antenna”, *IEEE Antennas and wireless propagation letters*, vol.10, pp.403-406, 2011.

14 K.H. Kim, Y.J. Cho, S.H. Hwang and S.O. Park, "Band-notched UWB planar monopole antenna with two parasitic patches”, *Electronics Letters*, vol.41, pp.783-785, July 2005.

15 M. Ur-Rehman, Q.H. Abbasi, M. Akram, C. Parini, "Design of band-notched ultra wideband antenna for indoor and wearable wireless communications", *IET Microwaves, Antennas & Propagation*, vol. 9, no.3, pp.243 – 251, 2015.

This is a draft of the accepted Journal on IET MAP;
ISSN 1751-8725; August 2015
doi: 10.1049/iet-map.2014.0736
www.ietdl.org

16 H. Huang, Y. Liu, and S. Gong, "Uniplanar differentially driven UWB polarization diversity antenna with band-notched characteristics", *Electronics Letters*, vol.51, no.3, pp.206 - 207, 2015.

17 D. Sarkar, K. V. Srivastava, and K. Saurav, "A Compact Microstrip-Fed Triple Band-Notched UWB Monopole Antenna", *IEEE Antennas and Wireless Propagation Letters*, vol.13, pp.396-399, 2014.

18 L. Liu, S. W. Cheung, and T. I. Yuk, "Compact MIMO Antenna for Portable UWB Applications with Band-Notched Characteristic*," IEEE Transactions on Antennas and Propagation*, vol.63, no.5, pp.1917 - 1924, 2015.

19 R. L. Haupt, and D. H. Werner, "Genetic Algorithms in Electromagnetics", IEEE Press Wiley-Interscience, 2007.

20 J. Robinson and Y. Rahmat-Samii, “Particle Swarm Optimization in Electromagnetics”, *IEEE Transactions on Antennas & Propagation*, vol.52, no.2, pp. 397-407, February 2004.

21 W.C. Liu, “Design of a Multiband CPW-fed Monopole Antenna Using a Particle Swarm Optimization Approach”, *IEEE Transactions on Antennas & Propagation*, vol.53, no.10, pp.3273-3279, October 2005.

22 X. S. Yang, “Multi-objective firefly algorithm for continuous optimization”, *Engineering with Computers*, vol.29, no.2, pp.175-184, 2013.

23 Eberhart and Kennedy, "Particle Swarm Optimization”, *IEEE International Conference on Neural Networks*, 1995.

24 X. S. Yang, “Firefly algorithms for multimodal optimization", Proceedings of the 5th International Conference on Stochastic Algorithms: Foundations and Applications, SAGA 2009, LNCS-Springer, vol.5792, pp.69-178, 2009.

25 MATLAB: Mathematics Lab, “The Language of Technical Computing”, Ver.7.8.0.347, Mathworks, 2013.

This is a draft of the accepted Journal on IET MAP;
ISSN 1751-8725; August 2015
doi: 10.1049/iet-map.2014.0736
www.ietdl.org

26 “CST: Computer Simulation Technology Based on FIT Method”, CST Computer Simulation Technology, 2014.